Proximity Relationship between the Active Site of *Escherichia coli* RNA Polymerase and Rifampicin Binding Domain: A Resonance Energy-Transfer Study†

K. Prasanna Kumar, Padmalatha S. Reddy, and Dipankar Chatterji*

Centre for Cellular and Molecular Biology, Uppal Road, Hyderabad 500 007 (A.P.), India

Received March 17, 1992; Revised Manuscript Received May 26, 1992

ABSTRACT: *Escherichia coli* RNA polymerase has two subsites, *i* and *i* + 1, for the binding of the first two substrates, and the first phosphodiester bond is formed between them during the initiation of transcription. Various studies have shown earlier that the inhibitor rifampicin has little effect, if any, on the formation of this phosphodiester bond. On an earlier occasion, we measured the distance of the *i* nucleotide from the rifampicin binding site on RNA polymerase using Forster's energy-transfer mechanism [Kumar & Chatterji (1990) *Biochemistry 29*, 317]. In this paper, the 1-aminonaphthalene-5-sulfonic acid (AmNS) derivative of UTP in the presence of 10 mM $MgCl_2$ was used as an energy donor, and its distance from rifampicin was estimated. The modified nucleotide (γ-AmNS)-UTP binds to RNA polymerase with a K_d of 3 μM and has one binding site in the presence of Mg(II) ion. Fluorescence titration studies performed with or without an initiator indicated that (γ-AmNS)-UTP exclusively binds to RNA polymerase at the (*i* + 1) site in the presence of Mg(II). Rifampicin was found to form a 1:1 complex with RNA polymerase bound to labeled UTP. Rifampicin and (γ-AmNS)-UTP have a substantial spectral overlap with an energy-transfer efficiency close to 50%. Labeled UTP shows a decrease in its excited-state lifetime when bound to the enzyme; the transfer efficiency calculated from lifetime measurements was found to be lower than that estimated from steady-state spectral analysis. Time-resolved emission spectral analysis was carried out to differentiate between the free and bound UTP over the enzyme surface. Bound UTP showed rapid decay in the presence of the acceptor within 5 ns. The rotational correlation time of the bound probe was estimated to be less than the lifetime of its excited state, indicating that substantial rotation of the donor can occur during its decay. The distance between the donor and the acceptor was estimated to be around 20 Å, using Forster's theory of dipole–dipole energy transfer. A model has been proposed where the distances of both *i* and (*i* + 1) nucleotides from rifampicin have been fixed, considering they are suitably oriented for phosphodiester synthesis. From this model it becomes apparent how rifampicin could block the translocation event during transcription initiation without hindering the first phosphodiester synthesis.

Escherichia coli RNA polymerase is a large multisubunit enzyme ($\alpha_2\beta\beta'\sigma$) with an approximate molecular weight of 450 000. It has two tightly bound Zn atoms per molecule of protein (Wu & Wu, 1981). RNA polymerase brings together two substrates for internucleotide bond formation at the active site of the enzyme in a template-dependent fashion. Various structural analyses carried out so far have suggested that one of the substrate binding sites is template independent and purine nucleotide specific, and later it was designated the initiation site of the enzyme (Chatterji & Wu, 1982a). This site is located very close to one of the Zn atoms, suggesting a possible role of Zn in catalytic function of the enzyme (Chatterji & Wu, 1982b; Chatterji et al., 1984). On the other hand, the second site is Mg(II) ion dependent and shows no nucleotide preference. These two substrate binding sites of *E. coli* RNA polymerase are also called the *i* and (*i* + 1) sites (Yager & von Hippel, 1988). Formation of the first phosphodiester bond between the *i* nucleotide and the (*i* + 1) nucleotide marks the initiation of transcription and, therefore, controls the regulation of RNA synthesis. Although the other Zn(II) atom is located at the β'-subunit (Miller et al., 1979), which has a putative Zn-finger motif (Chatterji & Guruprasad, 1988), its exact function in template recognition or elongation of RNA chains still remains elusive. Recently, with the help of a series of magnetic resonance measurements, Eichhorn and his colleagues have determined the geometric relationship between two substrates bound to RNA polymerase (Chuknyisky et al., 1990; Beal et al., 1990). Thus, from all of the studies mentioned above, a clearer picture of the catalytic synthesis of the first phosphodiester bond is slowly emerging.

It is known that the rifampicin class of antibiotics inhibit the initiation of transcription in *E. coli* (Sippel & Hartmann, 1968). The rifampicin binding domain is located in the β-subunit of the enzyme (Bahr et al., 1976; Gurgo, 1980) and is about 30 Å away from the *i* site of RNA polymerase as measured recently by resonance energy-transfer study (Kumar & Chatterji, 1990). This essentially suggests that rifampicin-induced inhibition of transcription initiation is noncompetitive with the *i* or initiating substrate. Furthermore, McClure and Cech (1978) reported that the major effect of rifampicin is a total block of the translocation step that would ordinarily follow the formation of the first phosphodiester bond. The initiation phase of transcription in *E. coli* can be further subdivided into the following discrete steps: (i) formation of the open complex between DNA and RNA polymerase; (ii) stabilization of the initiating ternary complex after the synthesis of the first few phosphodiester bonds; (iii) release of σ-factor and conversion of the initiating ternary complex into an elongating complex. The action of rifampicin is thought to be primarily on the steps subsequent to the

† This project was partly funded by the Department of Science and Technology, Government of India.

* Author to whom correspondence should be addressed (fax 91-842-851195).

0006-2960/92/0431-7519$03.00/0 © 1992 American Chemical Society

formation of the first phosphodiester bond (Krummel & Chamberlin, 1989; Mishra & Chatterji, 1991; Kumar & Chatterji, 1992). This raises an important question regarding the spatial disposition of this inhibitor with respect to the two substrates at the i and $(i + 1)$ sites during the first phosphodiester synthesis. Ideally, one should saturate both the i and $(i + 1)$ sites with substrates and then measure their respective distances from rifampicin when both substrates are suitably oriented for bond formation. It has been demonstrated that the latter condition can be achieved in the absence of a template as the orientation of the $(i + 1)$ nucleotide in the presence or absence of template remains more or less the same (Wu & Tyagi, 1987; Beal et al., 1990). In addition, the absence of a template ensures the formation of enzyme–substrate complex without turning the product over. However, experimental constraints limit any spectroscopic measurements when both substrate binding sites of RNA polymerase are saturated with nucleotides. Therefore, in this study we have attempted to formulate the proximity of rifampicin in the presence of Mg(II) with $(i + 1)$ nucleotide when the latter was tagged with a fluorescent reporter molecule, using the method of energy transfer. The geometry of the active site and its spatial disposition with respect to rifampicin were mapped with the knowledge of the distance of the i nucleotide from this inhibitor (Kumar & Chatterji, 1990).

EXPERIMENTAL PROCEDURES

Materials. Rifampicin and nucleotides were purchased from Sigma and Boehringer Manheim, respectively. The quality of the triphosphates was checked by thin-layer chromatography on poly(ethylene imine) (PEI) plates as described before (Schleif & Wensink, 1981). All other routine chemicals were of purest grade available. Radionucleotides used for the RNA polymerase assay were the product of Amersham and Bhabha Atomic Research Centre, Bombay, India.

Methods. E. coli RNA polymerase was purified from mid-log phase cells of a RNaseI$^-$ strain (MRE600) essentially following the method of Burgess and Jendrisak (1975) but with a modification developed in this laboratory (Kumar & Chatterji, 1988). Sodium dodecyl sulfate–polyacrylamide gel electrophoretic (SDS–PAGE) analysis showed that the enzyme was 98% pure. The enzyme was found to have more than 60% active molecules with specific activity 2500 units/mg.

Fluorescence Labeling of UTP. Fluorescence labeling of UTP with 1-aminonaphthalene-5-sulfonate (AmNS) via a γ-phosphoramidate bond was essentially achieved following the protocol described before (Yarbrough et al., 1979). The same authors reported earlier, as did Wu and Tyagi (1987), that (γ-AmNS)-UTP acts as a very good substrate for *E. coli* RNA polymerase. It has a fluorescence emission maximum at 460 nm when excited at 340 nm.

Fluorescence Studies. All steady-state fluorescence and lifetime experiments were performed in a buffer containing 40 mM Tris-HCl (pH 7.9), 10 mM $MgCl_2$, 50 mM KCl, and 0.2 mM dithiothreitol. Steady-state spectral measurements were carried out in a Hitachi F-4000 spectrofluorometer with spectral correction. The absorption of the samples at the excitation wavelength was kept low so as to avoid inner-filter effect. All spectral measurements were done at 24 °C with constant slit of 5-nm bandpass.

Quantum Yields of the Samples. Quantum yields (Q_d) of samples were calculated from the corrected emission spectra of the reference and sample following eq 1 (Chen, 1965; Wu & Tyagi, 1987). The subscripts s and d represent standard reference and sample, respectively. A represents absorbance

$$Q_d = Q_s \frac{\int F_d \Delta\lambda}{\int F_s \Delta\lambda} \frac{q_s}{q_d} \frac{A_s}{A_d} \quad (1)$$

at the excitation wavelength, which was always <0.1 to reduce inner-filter quenching. F is the relative fluorescence intensity, and $\Delta\lambda$ is the wavelength interval over which integration was carried out. q equals relative photon output of the source at the excitation wavelength at constant slit opening. Quinine sulfate in 1 N H_2SO_4 was used as standard ($Q_s = 0.7$) (Valapoldi & Mielenz, 1978).

Measurement of the Distance between Donor and Acceptor by Forster's Theory (Forster, 1948). In our case, the donor was (γ-AmNS)-UTP–RNA polymerase and the acceptor was rifampicin. As rifampicin absorbs strongly in the 330–340-nm region, we excited the donor at 360 nm both in the presence and in the absence of rifampicin. This resulted in a reduced quantum yield of the donor at the emission maximum of 460 nm. Rifampicin also has an absorption band around 460 nm.

In the Forster theory of dipole–dipole energy transfer, the transfer efficiency, E, is related to the distance, r (angstroms), between the donor and the acceptor by

$$r = R_0(1/(E-1))^{1/6} \quad \text{or} \quad E = r^{-6}/(r^{-6} + R_0^{-6}) \quad (2)$$

Transfer efficiency can also be written as

$$E = 1 - (\tau_a/\tau_0) \quad (3)$$

when mτ_a and τ_0 are the excited-state lifetimes of the donor in the presence (τ_a) and absence (τ_0) of the acceptor. E can also be calculated from

$$E = 1 - (Q_a/Q_0) \quad (4)$$

where Q_a and Q_0 represent quantum yields of donor in the presence (Q_a) or absence (Q_0) of the acceptor. R_0, the distance between donor and acceptor (angstroms) at which the transfer efficiency equals 50%, is given by

$$R_0 = 9.79 \times 10^3[(J)(Q_a)(n^{-4})(\kappa)^2]^{1/6} \quad (5)$$

where J, the spectral overlap integral between the emission spectrum of the donor and the absorption spectrum of the acceptor, is

$$J = \int F_d(\lambda)\epsilon_a(\lambda)\lambda^4\Delta\lambda / \int F_d(\lambda)\Delta\lambda \quad (6)$$

where $F_d(\lambda)$ and $\epsilon_a(\lambda)$ are the relative fluorescence intensity (percent) of the donor and the molar extinction coefficient (M^{-1} cm^{-1}) of the acceptor, respectively, and λ is the wavelength at nanometer interval, $\Delta\lambda$. A FORTRAN program to calculate J has been reported earlier (Kumar & Chatterji, 1990). In eq 5, n is the refractive index of the medium between donor and acceptor and was taken as 1.4. An uncertainity always arises from the estimation of the value for κ^2, the orientation factor of both donor and acceptor, which is discussed under Results.

Time-Resolved Emission Spectroscopy of the Donor in the Presence and Absence of the Acceptor. All time-resolved fluorescence intensity decays were measured in the stroboscopic system of a Photon Technology International (Canada) LS-100 luminescence spectrometer. It employs a thyratron-gated nanosecond flash lamp filled with nitrogen having pulse width of less than 1.6 ns. The manufacturer-supplied nonlinear least-squares fitting program was used for single-exponential or multiexponential decay fittings and for the estimation of preamplitude and lifetime values. It involves deconvolution by iterative reconvolution (O'Connor & Phillips, 1984), and

the program includes a statistical and plotting subroutine package. Statistical tests include Chi-square, the Durbin–Watson test, the covariance matrix, a runs test, and the autocorrelation function. Time-resolved emission spectra (TRES) were recorded by acquiring a series of fluorescence decays over a range of emission wavelengths, and the TRES were then reconstructed the same way as mentioned above, from deconvoluted decay curves. Computer drawing of the stereo model was carried out using the Macro-model 2.5 program available at Bioinformatics Centre, CCMB, Hyderabad.

Fluorescence Anistropy and Rotational Correlation Time. For a polarized light, the time dependence of fluorescence may be calculated from the raw data

$$F(t) = I(t)_{par} + 2GI(t)_{per} \quad (7)$$

where $I(t)_{par}$ is the intensity of light detected with a vertical excitation polarizer and a vertical emission polarizer, $I(t)_{per}$ is the intensity of light detected with a vertical excitation polarizer and a horizontal emission polarizer, and G is the correction term for the relative throughput of each polarization through the emission optics.

Time-dependent anisotropy, $r(t)$, is defined as

$$r(t) = \frac{I(\text{par}) - GI(\text{per})}{I(\text{par}) + 2GI(\text{per})} = \frac{d(t)}{F(t)}$$

This function is known to decay with a multiexponential decay law (Phillips et al., 1985).

$$r(t) = \sum_{i=1}^{5} b_i \exp(-t/\phi_i) + b_\infty \quad (8)$$

Although the sum can run to five terms for completely anisotropic rotational motion, at lower precision levels and with relatively symmetric rotors, eq 8 will only yield in practice one or two terms. The b_∞ term refers to residual anistropy remaining after all of the transient terms have decayed and is commonly interpreted to imply restricted motion of the rotor. The term ϕ_i denotes rotational correlation time. It can be solved by convolution technique. Noting that

$$d(t) = r(t)F(t) = I(\text{par}) - GI(\text{per}) \quad (9)$$

it can be written

$$d(t) = [\sum_i a_i \exp(-t/\tau_i)][\sum_j b_j \exp(-t/\phi_j) + b_\infty] \quad (10)$$

where a_i and τ_i denote amplitude and lifetime of the excited state. Once a_i and τ_i are solved from the decay curves, they can be used as constants and values for ϕ and b can be obtained by iteration.

RESULTS

Binding of (γ-AmNS)-UTP to E. coli RNA Polymerase. It has been reported earlier that the fluorescence-labeled UTP acts as a substrate for *E. coli* RNA polymerase (Yarbrough et al., 1979; Wu & Tyagi, 1987). The K_d for (γ-AmNS)-UTP to the enzyme had been reported to be 3.6 μM. However, in this case the titration was carried out by keeping the probe concentration constant and varying the enzyme concentration over a wide range. Occasionally, this gives an erroneous estimation of K_d values due to the presence of a large amount of protein in the optical path, resulting in frothing and scattering. Thus, we decided to estimate the dissociation constant by keeping the enzyme at low fixed concentration and varying the probe. RNA polymerase was excited at 295 nm, where the probe shows minimal absorption, and tryptophan emission at 340 nm was monitored as shown in Figure 1a. When the intensity of the tryptophan emission was plotted against (γ-AmNS)-UTP (Figure 1b), the K_d value was estimated to be around 3 μM from the half-maximal saturation of the titration curve in Figure 1b, and this value is in close agreement with that reported earlier. On the basis of this K_d value, we estimate about 90% of the enzyme to be in the complexed form. Moreover, upon incremental addition of (γ-AmNS)-UTP to the enzyme, an isoemissive point was observed at 380 nm (Figure 1a), indicating the presence of only one type of complex between (γ-AmNS)-UTP and RNA polymerase. After the binding parameters for (γ-AmNS)-UTP and *E. coli* RNA polymerase were established, the subsequent fluorescence studies were carried out with low substrate (0.4 μM) and excess enzyme concentrations (8 μM), so that at least 70% of the labeled substrate was in complex form.

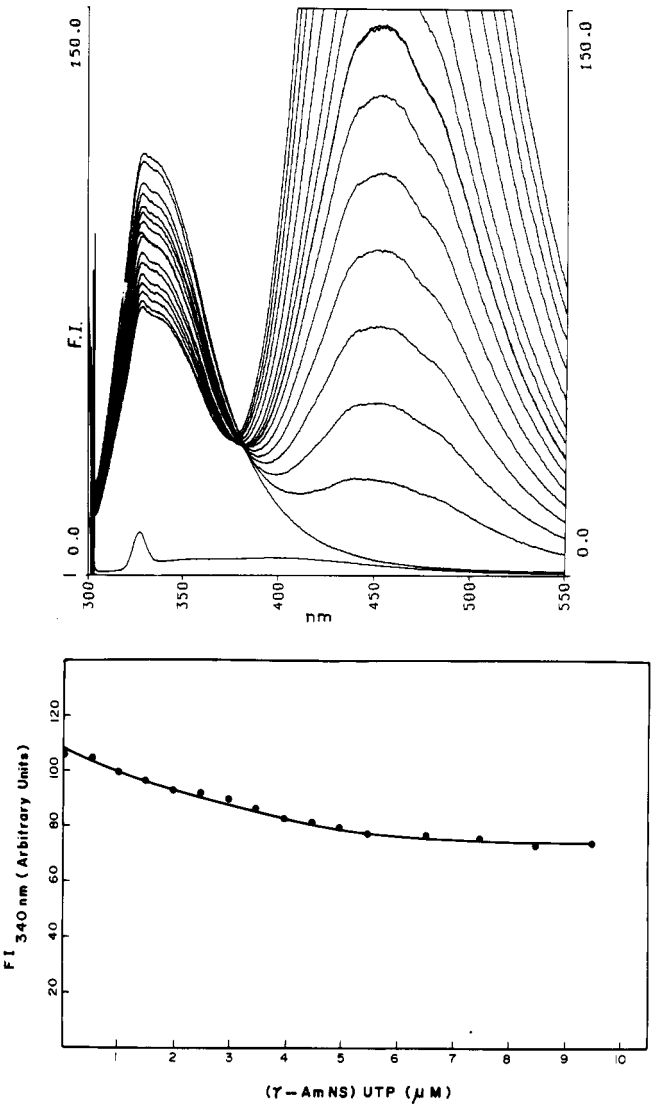

FIGURE 1: Fluorescence quenching of the tryptophan emission of *E. coli* RNA polymerase (0.1 μM) when excited at 295 nm with various amounts of (γ-AmNS)-UTP, in a buffer containing 80 mM Tris-HCl (pH 7.9), 10 mM $MgCl_2$, 50 mM KCl, and 0.2 mM dithiothreitol. (a, top) F.I. stands for fluorescence arbitrary intensity, whereas nm is the wavelength in nanometers. The base line shows a band at 320 nm due to Raman emission. Development of the 460-nm band due to (γ-AmNS)-UTP can be noticed due to incremental addition. (b, bottom) Titration of the tryptophan emission at 340 nm is plotted against the concentration of (γ-AmNS)-UTP as shown in (a).

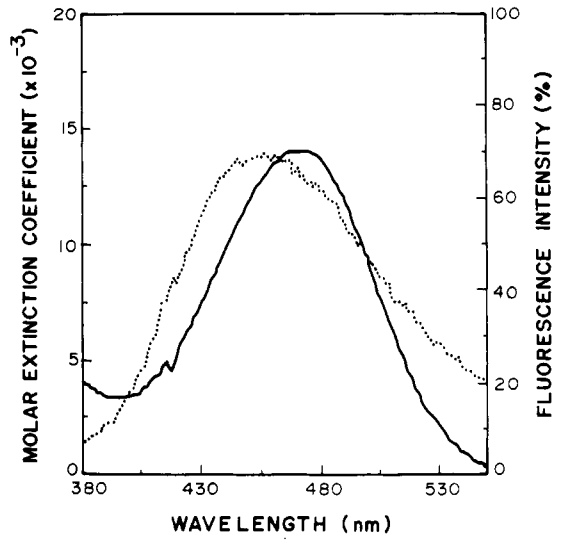

FIGURE 2: Spectral overlap between the absorption spectrum of rifampicin (—) and the corrected fluorescence emission spectrum of (γ-AmNS)-UTP–RNA polymerase (···).

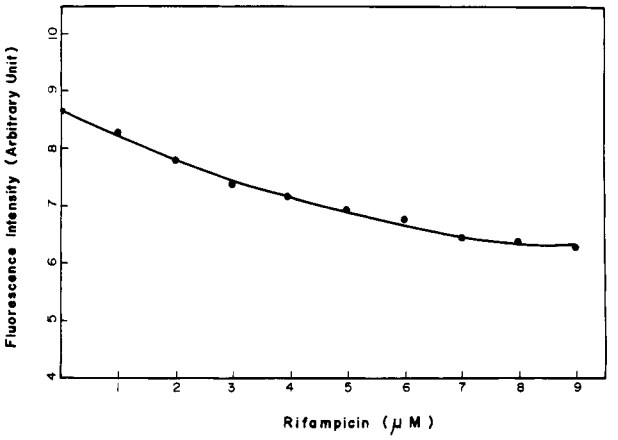

FIGURE 3: Titration of the corrected fluorescence emission of (γ-AmNS)-UTP–RNA polymerase with various concentrations of rifampicin at 460 nm when excited at 360 nm. The concentration of (γ-AmNS)-UTP was 0.4 μM, and that of RNA polymerase was 8 μM. The reaction was carried out in the same buffer as in Figure 1.

One needs to establish the binding site of (γ-AmNS)-UTP with *E. coli* RNA polymerase before one can proceed to estimate geometric distances. We have mentioned earlier that the Mg(II) complex of unlabeled UTP binds to the (i + 1) site of RNA polymerase. Similarly, it has been shown recently (Jin & Gross, 1991) that (γ-AmNS)-UTP can be used in place of UTP during abortive synthesis of pppApU at $\lambda P_{R'}$ promoter; the synthesis of dinucleotide can be monitored by the change in fluorescence emission.

Further proof that (γ-AmNS)-UTP in the presence of Mg(II) binds to the (i + 1) site of RNA polymerase comes from fluorescence titration experiments. The quenching of the tryptophan emission (see Figure 1) of RNA polymerase with various (γ-AmNS)-UTP showed a similar profile when an excess of UMP was present in the medium. With an idea that nucleoside monophosphates cannot bind to the (i + 1) site but can, however, be used as initiator (i site) in RNA synthesis, the above experiment suggested that even when the i site is occupied, (γ-AmNS)-UTP binds RNA polymerase at i + 1 in the presence of Mg(II). Nucleoside monophosphate UMP is known to have no effect on the tryptophan fluorescence of RNA polymerase as reported earlier (Wu & Goldthwait, 1969). Thus, the above experiment was carried out by saturating the enzyme with UMP and then titrating the resulting emission with various (γ-AmNS)-UTP in the presence of Mg(II). This along with the observations mentioned earlier that (γ-AmNS)-UTP titration of *E. coli* RNA polymerase showed one isoemissive point with binding stoichiometry 1:1 strongly suggests its binding to the (i + 1) site. Further evidence came from time-resolved emission spectroscopic analysis mentioned in the later section.

Binding of Rifampicin to (γ-AmNS)-UTP–RNA Polymerase Complex. Rifampicin has two absorption peaks in the visible region (Bahr et al., 1976). The peak absorbing at the longer wavelength has a substantial spectral overlap with the (γ-AmNS)-UTP–RNA polymerase emission maximum as shown in Figure 2. Therefore, in principle, it can form a Forster donor–acceptor pair with labeled UTP when both are bound to RNA polymerase and suitably placed. It was indeed observed that, upon addition of rifampicin to (γ-AmNS)-UTP–RNA polymerase, the emission of the reporter molecule was progressively quenched as shown in Figure 3. As expected, the titration curve approached saturation when the enzyme to rifampicin ratio approached unity. It should be mentioned here that, due to the strong absorption of rifampicin around 330 nm, (γ-AmNS)-UTP was routinely excited at 360 nm in all subsequent steady-state studies both in the presence and in the absence of rifampicin. In this way the inner-filter effect due to the presence of rifampicin could be avoided. It was noticed earlier that rifampicin shows minimal absorption at 360 nm (Bahr et al., 1976) and, therefore, this is the region of choice for excitation, particularly when a considerable amount of rifampicin is present in the medium. Such off-maximal excitation also reduced the quantum yield of the donor as shown in Table I.

Lifetime and Time-Resolved Emission Spectra (TRES) of the Donor in the Presence and Absence of Acceptor. Figure 4 shows the decay profile of free (γ-AmNS)-UTP when excited at 337 nm, corresponding to the nitrogen absorbing line. Table II list the lifetime values obtained for labeled UTP when complexed with RNA polymerase in the presence and absence of rifampicin. These values are an average of at least three independent measurements. The fluorescence decays were deconvoluted with the instrument response function and fitted to theoretical decay functions with a nonlinear least-squares fitting program based on the Marquardt algorithm (Press et al., 1986). The accuracy of fits was judged by the χ^2 criterion, and the plots of the weighted residuals as well as autocorrelation are shown in Figure 4 (O'Connor & Phillips, 1984). The χ^2 value in each case varied between 0.85 and 1.2. All of the samples that were measured and reported in Table II were best fitted with two exponentials, one of them with a lifetime of a few hundred picoseconds and negligible amplitude. As a consequence, the contribution from this component was not appreciable in the total fluorescence intensity and could be neglected. It can be noticed from Table II that (γ-AmNS)-UTP has an appreciably long lifetime, similar to that reported before for (γ-AmNS)-ATP (20 ns) (Yarbrough et al., 1979). Interestingly, upon complexation with RNA polymerase, the lifetime of the probe is substantially reduced.

Figure 5a shows the time-resolved emission spectra of (γ-AmNS)-UTP when complexed with RNA polymerase. In the time axis the spectra obtained in the first 2 ns after the pulse are not shown since the deconvolution is subject to error at early time points. Two distinct emission peaks were observed, one around 460 nm and the other around 445 nm. Resolution of the emission maximum in two different peaks

Table I: Spectral Overlap Integral between Donor [(γ-AmNS)-UTP–RNA Polymerase] and Acceptor Rifampicin, Quantum Yield of Donor, Energy-Transfer Efficiencies, Various Excitation and Emission Wavelengths, and Distance between Donor and Acceptor in (γ-AmNS)-UTP–RNA Polymerase and Rifampicin Complex

sample	excitation wavelength (nm)	emission wavelength (nm)	spectral overlap integral, J (M^{-1} cm^3)	quantum yield, Q	distance at 50% energy-transfer efficiency, R_0 (Å)	energy-transfer efficiency, E	distance between donor and acceptor (Å)
(γ-AmNS)-UTP[a]	340	460		0.0860			
(γ-AmNS)-UTP–RNA polymerase	360	460		0.0043			
(γ-AmNS)-UTP–RNA polymerase–rifampicin (9 μM)	360	460	5.13×10^{-14}	0.0020	18.0	0.53	17.6

[a] Taken from Yarbrough et al. (1979). Concentrations of (γ-AmNS)-UTP and RNA polymerase were 0.4 and 8 μM, respectively.

Table II: Lifetimes, Energy-Transfer Efficiencies, and Distance between Donor and Acceptor in (γ-AmNS)-UTP–RNA Polymerase–Rifampicin Complex[a]

sample	lifetime (ns)	energy-transfer efficiency, E	distance between donor and acceptor (Å)
(γ-AmNS)-UTP	11.10 ± 0.500		
(γ-AmNS)-UTP–RNA polymerase	6.32 ± 0.020		
(γ-AmNS)-UTP–RNA polymerase–rifampicin (9 μM)	3.72 ± 0.005	0.41	19.1

[a] Excitation wavelength was 337 nm, corresponding to the peak in nitrogen lamp. Concentrations of (γ-AmNS)-UTP and RNA polymerase were 0.4 and 8 μM, respectively.

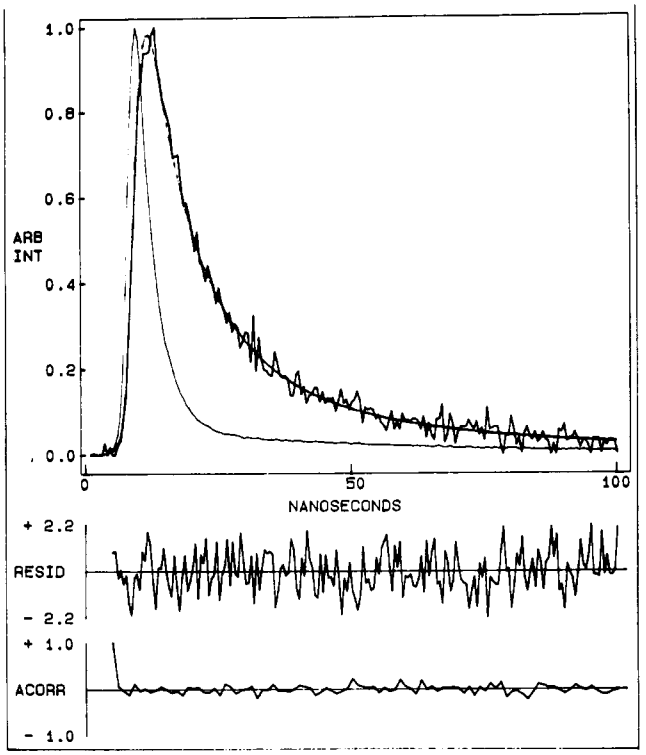

FIGURE 4: Fluorescence decay of (γ-AmNS)-UTP when excited at 337 nm corresponding to the lamp peak. Emission wavelength was 460 nm. The bottom two curves show the weighted residual and autocorrelation analysis.

on the time axis may have its origin either in ground-state heterogeneity or in excited-state interaction (Badea & Brand, 1979). It should be mentioned here that TRES of free (γ-AmNS)-UTP with Mg(II) showed a broad emission peak centered around 460 nm (not shown) with a minor component at higher wavelength. In addition, the concentrations of (γ-AmNS)-UTP and RNA polymerase were 0.4 and 8 μM, respectively. With a K_d value of 3 μM, it can be estimated that about two-thirds of the (γ-AmNS)-UTP stayed as a complex with RNA polymerase, whereas the other one-third remained free. In addition, results of Figure 1 show that the (γ-AmNS)-UTP binds as a 1:1 complex with the enzyme in the presence of Mg(II). Therefore, in all probability, the resolution of the emission maximum in this case (Figure 5a) is due to the ground-state heterogeneity; we are tempted to assign the peak around 460 nm to the free probe and the other one at 445 nm to the bound one. The shift of the band of the bound probe to higher energy indicates a more hydrophobic environment, as expected. That the higher wavelength emission maximum is due to free (γ-AmNS)-UTP was further evidenced from the competition experiment shown in Figure 5b. When excess of unlabeled UTP was added to (γ-AmNS)-UTP–RNA polymerase complex, the signal due to the free labeled UTP was completely quenched in comparison to that of bound one. Such would be the case if the bound probe was less accessible to environment.

Figure 5c shows the TRES recorded when 9 μM rifampicin was added to the (γ-AmNS)-UTP–RNA polymerase complex having the same concentration as in Figure 5a. With an estimated K_d of 1 nM between those of rifampicin and RNA polymerase (Wehrli, 1977), it can be calculated that almost 100% of the enzyme and 90% of rifampicin can be reckoned to be in the complex form. One may notice from Figure 5a,c that the peak at 445 nm, due to the complexed UTP, is shifted to lower energy in both cases, probably due to excited-state solvent interaction (Lakowicz, 1983). This is fairly a common phenomenon in TRES as also noticed for the free UTP around 460 nm in the absence of rifampicin (Figure 5a). Interestingly, upon addition of rifampicin, a rapid decay of the complexed UTP (Figure 5c) at 445 nm was observed without any other change, and we attributed this decay to the dipolar energy transfer through Forster's mechanism. It should be mentioned here that if the TRES reported in Figure 5a,c are interpreted as due to the ground-state heterogeneity of (γ-AmNS)-UTP, then the lifetimes shown in Table II are expected to have contribution from both the free and bound UTP.

Calculation of the Distance between (γ-AmNS)-UTP and Rifampicin When Both Are Bound to RNA Polymerase. Rifampicin is known to form a 1:1 stoichiometric complex with *E. coli* RNA polymerase (Gurgo, 1980) with a binding constant of 1×10^9 M^{-1} (Wehrli, 1977). Although the rifampicin binding domain has been located on the β-subunit (Kumar & Chatterji, 1990), it appears that the proper juxtaposition of four segments of β-subunit is necessary for the creation of the rifampicin binding site (Jin & Gross, 1988), which requires the assembly of core RNA polymerase ($\alpha_2\beta\beta'$). We also observed the formation of a 1:1 complex between (γ-AmNS)-UTP–RNA polymerase and rifampicin in the presence of 10 mM $MgCl_2$ as shown in Figure 3.

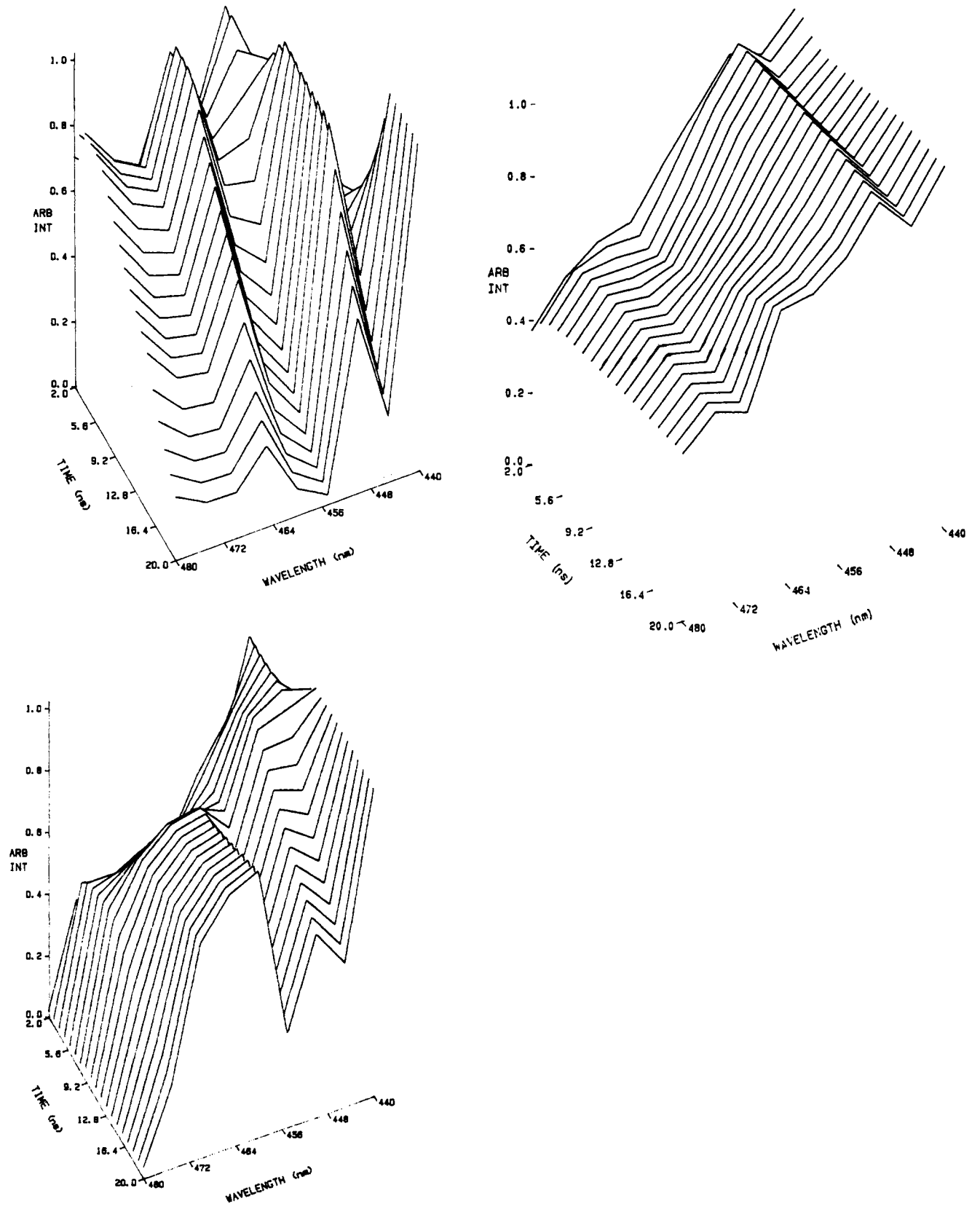

FIGURE 5: Time-resolved emission spectroscopic analysis of (γ-AmNS)-UTP–RNA polymerase (a, top left) and that in the presence of 1 mM unlabeled UTP (b, top right) or a stoichiometric amount of rifampicin (c, bottom left). Please see text for details. Excitation was carried out in this case at 337 nm, corresponding to the nitrogen absorbing line. The reaction buffer was the same as in Figure 1. In each case the residuals and autocorrelation functions were checked.

It can be seen from Tables I and II that we attempted to calculate transfer efficiency both from quantum yield and from lifetime values. Both methods assume that the insertion of the acceptor does not alter the quantum yield of the donor except by the energy-transfer process itself (Stryer, 1978). We also noticed a discrepancy in the transfer efficiencies calculated from different methods. However, it has been mentioned before (Hard et al., 1989) that the transfer efficiency values obtained from steady-state measurements are more reliable than those measured from lifetime exper-

Table III: Lifetime (τ) and Rotational Correlation Time (τ_r) of (γ-AmNS)-UTP–RNA Polymerase in the Presence and Absence of Rifampicin

sample	τ (ns)	τ_r (ns)
(γ-AmNS)-UTP	11.10 ± 0.500	1.97 ± 0.50
(γ-AmNS)-UTP–RNA polymerase	6.32 ± 0.020	2.77 ± 0.90
(γ-AmNS)-UTP–RNA polymerase–rifampicin	3.72 ± 0.005	2.08 ± 0.01

iments. In addition, the estimation of the lifetime of bound (γ-AmNS)-UTP may be in error due to the contribution from free (γ-AmNS)-UTP as stated before. On the other hand, transfer efficiency calculated from steady-state measurements was corrected for unbound probe. Moreover, taking the error limit of lifetime values in distance approximation, both methods yielded proximity of donor and acceptor within the agreeable range, and thus we did not attempt to determine the reason behind such discrepancy in energy-transfer efficiency.

It is well-known that one of the major sources of error in fluorescence resonance energy-transfer measurements is the estimation of the orientation factor, κ^2 (Stryer, 1978; Dale & Eisinger, 1976). If either the donor or the acceptor is freely moving or isotropic in nature, then the value $^2/_3$ is used for κ^2. However, if the donor or the acceptor or both are attached to a macromolecule, then it may happen that they are fixed in a constant orientation to each other due to restricted rotation. In that case κ^2 can take a range of values between 0 and 4 depending upon the orientation. As the donor (γ-AmNS)-UTP in our case is bound to a large protein molecule, it was necessary to check its rotational freedom. Hence, we estimated the values of rotational correlation time (τ_r) from time-dependent anisotropy experiments, and these are reported in Table III. It can be seen from Table III that in all cases τ_r was less than the excited-state lifetimes, indicating that substantial rotation of the labeled substrate can occur during its decay. We have recently noticed that a similar observation made by others was interpreted as energy emission from an isotropic donor (Kim et al., 1991). Moreover, none of the cases listed in Table III had any residual anistropy b_∞ value during iterative fitting, indicating more or less free rotation of the donor. Nevertheless, it should be kept in mind that rifampicin, the acceptor, is noncovalently attached in a very tight fashion to a single site on the enzyme and thus may have an unknown fixed orientation which cannot be measured.

Thus, assigning a value of $^2/_3$ to κ^2, we calculated Forster's distance between (γ-AmNS)-UTP and rifampicin when both were bound to *E. coli* RNA polymerase with the help of eqs 1–6. These are reported in Tables I and II.

DISCUSSION

The purpose of this study was to determine the proximity of the first phosphodiester bond between i and (i + 1) nucleotides on *E. coli* RNA polymerase from the inhibitor binding site on the enzyme. To this end, we have chosen to conduct our studies in a buffer solution containing magnesium ions, but in the absence of any template; this is because previous studies have shown that the Mg(II) complex of (i + 1) nucleotide binds RNA polymerase more or less with the same conformation and affinity either in the presence or in the absence of a template (Wu & Tyagi, 1987; Chuknyisky et al., 1990; Beal et al., 1990). The experiments performed here suggested that the (γ-AmNS)-UTP binds RNA polymerase to a single site that is i + 1 in the presence of Mg(II), just as UTP does. We have assumed that the orientation of the (γ-AmNS)-UTP is proper for the catalytic bond formation

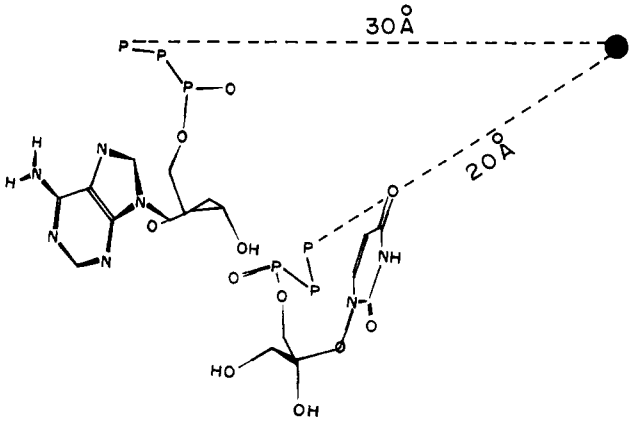

FIGURE 6: Schematic representation of the distance of rifampicin (●) from two nucleotides bound at the i site (purine) and the (i + 1) site (pyrimidine) of *E. coli* RNA polymerase. Orientation of the NTPs was first projected on a screen, keeping the distance of the 3′-OH (only hydroxyl shown) of the purine nucleotide within 2.5 Å of the α-phosphoryl of the pyrimidine nucleotide and the angle between 3′-OH (purine) and P_α–P_β (pyrimidine) to near linearity. The figure was then drawn and photographed.

with the nucleotide at the i position, and thus its distance measured from rifampicin probably represents the true distance. In addition, the absence of both template and nucleotide ensures the stabilization of the enzyme–substrate complex without any turning over of the product. We have earlier measured the distance of the i nucleotide from rifampicin, in the absence of (i + 1) nucleotide (Kumar & Chatterji, 1990), and observed in both cases that the presence of the second nucleotide obscures the spectroscopic signal from the first one either by absorption resulting in inner-filter quenching or by cross-contamination of signals in the region of interest. Hence, both of these studies were undertaken separately with either the i or (i + 1) nucleotide; in the following section we will try to interpret the results considering both are present in the system at the same time.

Figure 6 shows the geometric relationship between the i and (i + 1) nucleotides and the rifampicin binding domain. As suggested by Eichhorn and his colleagues (Beal et al., 1990), we have tried to draw this stereo model taking into account two points as the basis: (a) the distance of the i 3′-OH is within 2.5 Å of the (i + 1) α-phosphorus atom and poised for a nucleophilic attack; (b) the attacking and the leaving groups make an angle of 180° between them as appropriate for a SN_2 reaction. Regarding the mechanism of the first phosphodiester synthesis, it had been shown earlier (Yee et al., 1979) that the attack of the 3′-hydroxyl group of the i ATP upon the (i + 1) P α-atom and the release of pyrophosphate occur with an inversion of configuration at the phosphorus atom.

However, the actual angle we obtained from the stereo model between the attacking and leaving group was about 167°—still suitable for SN_2 mechanism. The distance of 30 Å between the γ-phosphorus of the i nucleotide and rifampicin, shown in Figure 6, was actually measured with a Tb(III) probe which binds to the phosphate group of GTP (Kumar & Chatterji, 1990). One of us had also shown earlier (Chatterji et al., 1984) that the i nucleotide undergoes conformational change in the presence of template DNA with a change in the position of its phosphate moiety. However, this change was found to be not very significant when compared to the large distance (30 Å) between the i nucleotide and rifampicin. Moreover, the 5′-terminal phosphate of the i nucleotide does not participate in the phosphodiester bond formation, and therefore

we did not try to determine the orientation of the *i* nucleotide with respect to rifampicin in the presence of a template.

Although the distance reported in this paper between the $(i + 1)$ site and rifampicin is about 18–19 Å, we assumed the said distance as 20 Å considering the maximum error limit of lifetime estimation toward transfer efficiency calculation. Similarly, the lower limit of this distance would be 17 Å as obtained from the steady-state measurements of energy-transfer efficiency (Table I). Beal et al. (1990) had earlier reported the active site geometry, and rifampicin could be placed in their model too, considering the distances measured by us. Nevertheless, we also noticed that the *i* and $(i + 1)$ NTPs are not parallel to each other, which may be a consequence of DNA unwinding that takes place during transcription initiation.

The striking feature which becomes apparent from Figure 6 is that the first phosphodiester bond is located away from the rifampicin binding site on RNA polymerase. The mechanistic implication of such an observation is manifold. First, it explains the apparent insensitivity of the first dinucleotide formation toward rifampicin as observed before (McClure & Cech, 1978). Second, Figure 6 also suggests a bias of the $(i + 1)$ nucleotide toward rifampicin over the *i* nucleotide. It implies that rifampicin has very little effect, if any, on the binding of *i* nucleotide to the enzyme. On the other hand, it would hinder progressively the binding of $(i + 1)$ or following nucleotides during the initiation phase of transcription like translocation, etc. It would be worthwhile to follow spectroscopically the distance geometry of the second phosphodiester bond from the rifampicin binding site.

ACKNOWLEDGMENT

We thank Dr. K. Gopalkrishna for his help in the computer drawing of Figure 6 and Drs. R. Nagaraj and D. Balasubramanian for reading the manuscript.

REFERENCES

Badea, M. G., & Brand, L. (1979) *Methods Enzymol. 61*, 378–425.

Bahr, W., Steder, W., Scheit, K. H., & Jovin, T. M. (1976) in *RNA Polymerase* (Losick, R., & Chamberlin, M., Eds.) pp 369–396, Cold Spring Harbor Laboratory, Cold Spring Harbor, NY.

Beal, R. B., Pillai, R. P., Chuknyisky, P. P., Leny, A., Tarien, E., & Eichhorn, G. L. (1990) *Biochemistry 29*, 5994–6002.

Burgess, R. R., & Jendrisak, F. F. (1975) *Biochemistry 14*, 4634–4638.

Chatterji, D., & Guruprasad, K. (1988) *Curr. Sci. 57*, 376–377.

Chatterji, D., & Wu, F. Y. H. (1982a) *Biochemistry 21*, 4651–4656.

Chatterji, D., & Wu, F. Y. H. (1982b) *Biochemistry 21*, 4657–4664.

Chatterji, D., Wu, C.-W., & Wu, F. Y.-H. (1984) *J. Biol. Chem. 259*, 284–289.

Chen, R. F. (1965) *Science 150*, 1593–1595.

Chuknyisky, P. P., Rifkind, J. M., Tarien, E., Beal, R. B., & Eichhorn, G. L. (1990) *Biochemistry 29*, 5987–5994.

Dale, R. E., & Eisinger, J. (1976) *Proc. Natl. Acad. Sci. U.S.A. 73*, 271–273.

Drushel, H. V., Sommers, A. L., & Cox, R. C. (1963) *Anal. Chem. 35*, 13–21.

Forster, T. (1948) *Ann. Phys. 2*, 55–75.

Gurgo, C. (1980) in *Inhibitors of DNA and RNA polymerases* (Sarin, P. S., & Gallo, R. C., Eds.) pp 159–189, Pergamon Press, Oxford, U.K.

Hard, T., Sayre, M. H., Geiduschek, E. P., & Kearns, D. R. (1989) *Biochemistry 28*, 2813–2819.

Jin, D. J., & Gross, C. A. (1988) *J. Mol. Biol. 202*, 45–58.

Jin, D. J., & Gross, C. A. (1991) *J. Biol. Chem. 266*, 14478–14485.

Kim, S. T., Heelis, P. F., Okamura, T., Hirata, Y., Mataga, N., & Sancar, A. (1991) *Biochemistry 30*, 11262–11270.

Krummel, B., & Chamberlin, M. J. (1989) *Biochemistry 28*, 7829–7842.

Kumar, K. P., & Chatterji, D. (1988) *J. Biochem. Biophys. Methods 15*, 235–240.

Kumar, K. P., & Chatterji, D. (1990) *Biochemistry 29*, 317–322.

Kumar, K. P., & Chatterji, D. (1992) *FEBS Letts.*, in press.

Lakowicz, J. R. (1983) *Principles of fluorescence spectroscopy*, Plenum Press, New York.

McClure, W. R., & Cech, C. L. (1978) *J. Biol. Chem. 253*, 8949–8956.

Miller, J. A., Serio, G. F., Howard, R. A., Bear, J. L., Evans, J. E., & Kimball, A. P. (1979) *Biochim. Biophys. Acta 579*, 291–297.

Mishra, R. K., & Chatterji, D. (1991) *Nucleosides Nucleotides 10*, 607–608.

O'Connor, D. V., & Phillips, D. (1984) in *Time-correlated single photon counting*, pp 180–189, Academic Press, Orlando, FL.

Phillips, D., Drake, R. C., O'Connor, D. V., & Cristensen, R. L. (1985) *Anal. Instrum. 14*, 267–292.

Press, W. H., Flannery, B. P., Teukolsky, S. A., & Vetterlin, W. T. (1986) in *Numerical recipes*, Chapter 14, Cambridge University Press, Cambridge, England.

Schlief, R. F., & Wensink, P. C. (1981) in *Practical methods in Molecular Biology*, pp 112–113, Springer-Verlag, New York.

Sippel, A., & Hartmann, G. (1968) *Biochim. Biophys. Acta 157*, 218–219.

Stryer, L. (1978) *Annu. Rev. Biochem. 47*, 819–846.

Velapoldi, R. A., & Mielenz, K. D. (1978) Abstract 102, 29th Pittsburgh Conference, Cleveland, OH.

Wehrli, W. (1977) *Eur. J. Biochem. 80*, 325–330.

Wu, C. W., & Goldthwait, D. A. (1969) *Biochemistry 8*, 4450–4458.

Wu, F. Y.-H., & Wu, C.-W. (1981) in *Advances in Inorganic Biochemistry* (Eichhorn, G. L., & Marzilli, L. G., Eds.) Vol. 3, pp 143–166, Elsevier/North-Holland, New York.

Wu, F. Y.-H., & Tyagi, S. C. (1987) *J. Biol. Chem. 262*, 13147–13154.

Yager, T. D., & von Hippel, P. H. (1988) in *Escherichia coli and Salmonella typhimurium: Cellular and Molecular Biology* (Neidhardt, F. C., Ed.) p 1241, American Society of Microbiology, Washington, DC.

Yarbrough, L. R., Schlageck, J. G., & Baughman, M. (1979) *J. Biol. Chem. 254*, 12069–12073.

Yee, D., Armstrong, V., & Eckstein, F. (1979) *Biochemistry 18*, 4116–4120.